Enzymatic Catalysis of Proton Transfer at Carbon: Activation of Triosephosphate Isomerase by Phosphite Dianion†

Tina L. Amyes and John P. Richard*

Department of Chemistry, University at Buffalo, State University of New York, Buffalo, New York 14260-3000

Received February 28, 2007

ABSTRACT: More than 80% of the rate acceleration for enzymatic catalysis of the aldose−ketose isomerization of (*R*)-glyceraldehyde 3-phosphate (GAP) by triosephosphate isomerase (TIM) can be attributed to the phosphodianion group of GAP [Amyes, T. L., O'Donoghue, A. C., and Richard, J. P. (2001) *J. Am. Chem. Soc. 123*, 11325−11326]. We examine here the necessity of the covalent connection between the phosphodianion and triose sugar portions of the substrate by "carving up" GAP into the minimal neutral two-carbon sugar glycolaldehyde and phosphite dianion pieces. This "two-part substrate" preserves both the α-hydroxycarbonyl and oxydianion portions of GAP. TIM catalyzes proton transfer from glycolaldehyde in D_2O, resulting in deuterium incorporation that can be monitored by ^1H NMR spectroscopy, with $k_{cat}/K_m = 0.26\ M^{-1}\ s^{-1}$. Exogenous phosphite dianion results in a very large increase in the observed second-order rate constant $(k_{cat}/K_m)_{obsd}$ for turnover of glycolaldehyde, and the dependence of $(k_{cat}/K_m)_{obsd}$ on $[HPO_3^{2-}]$ exhibits saturation. The data give $k_{cat}/K_m = 185\ M^{-1}\ s^{-1}$ for turnover of glycolaldehyde by TIM that is saturated with phosphite dianion so that the separate binding of phosphite dianion to TIM results in a 700-fold acceleration of proton transfer from carbon. The binding of phosphite dianion to the free enzyme ($K_d = 38$ mM) is 700-fold weaker than its binding to the fleeting complex of TIM with the altered substrate in the transition state ($K_d^{\ddagger} = 53\ \mu M$); the total intrinsic binding energy of phosphite dianion in the transition state is 5.8 kcal/mol. We propose a physical model for catalysis by TIM in which the intrinsic binding energy of the substrate phosphodianion group is utilized to drive closing of the "mobile loop" and a protein conformational change that leads to formation of an active site environment that is optimally organized for stabilization of the transition state for proton transfer from α-carbonyl carbon.

Despite the wealth of mechanistic and structural data available for enzyme catalysts of proton transfer at α-carbonyl carbon (*1*−*4*), the origins of the rate accelerations effected by these enzymes remain elusive. The principal burden for such enzymes is the very large thermodynamic barrier to the formation of simple enolates in aqueous solution (*5*−*7*), but the physical mechanism(s) by which they lower this barrier and the nature of the corresponding transition state stabilization remain topics of current interest.

Triosephosphate isomerase (TIM)[1] is the prototypical protein catalyst of proton transfer at α-carbonyl carbon and catalyzes the reversible stereospecific 1,2-shift of the *pro-R* proton at dihydroxyacetone phosphate (DHAP) to give (*R*)-glyceraldehyde 3-phosphate (GAP) by a single-base (Glu-165) mechanism through a *cis*-enediol(ate) intermediate (Scheme 1) (*8*). The early extensive studies of TIM provided a clear description of the chemical events that occur at the enzyme active site (*9*, *10*), and they show that the enzyme approaches "perfection" in its catalysis of the isomerization of triose phosphates (*11*).

TIM presents a unique opportunity for detailed study of the origin of the enzymatic rate acceleration for proton transfer at carbon for several reasons. (1) TIM catalyzes the aldose−ketose isomerization of small and chemically simple phosphodianion substrates, and it requires no cosubstrates, metal ions, or other cofactors (*8*−*10*). (2) The mechanism (*9*, *10*) and free energy profile (*11*) have been well-defined in extensive chemical (*12*−*14*), spectroscopic (*15*−*18*), kinetic (*19*−*23*), and isotope exchange (*8*, *11*, *24*−*27*) studies. (3) The overall canonical $(\beta,\alpha)_8$-barrel structure of the protein in which the active site lies at the C-terminal end of the barrel (*28*−*30*), the identity of the catalytic residues [principally the base Glu-165 and the electrophiles His-95 and Lys-12 (*9*, *10*)],[2] and the architecture of the active site have been characterized in extensive mutagenesis (*18*, *31*−*33*) and crystallographic (*34*−*44*) studies. (4) The importance of the 11-residue "mobile loop" (loop 6, Pro-166 to Ala-176) has been explored via crystallographic (*36*−*38*, *40*−*42*, *44*, *45*),

† This work was supported by Grant GM39754 from the National Institutes of Health.

* To whom correspondence should be addressed. Telephone: (716) 645-6800, ext. 2194. Fax: (716) 645-6963. E-mail: jrichard@chem.buffalo.edu.

[1] Abbreviations: TIM, triosephosphate isomerase; DHAP, dihydroxyacetone phosphate; GAP, (*R*)-glyceraldehyde 3-phosphate; *h*-GLY, glycolaldehyde; *d*-GLY, glycolaldehyde labeled with one deuterium at C2; NMR, nuclear magnetic resonance; GPDH, glycerol 3-phosphate dehydrogenase; BSA, bovine serum albumin; NADH, nicotinamide adenine dinucleotide, reduced form; D,L-GAP, D,L-glyceraldehyde 3-phosphate; PGA, 2-phosphoglycolic acid, sodium salt; OMPDC, orotidine 5′-monophosphate decarboxylase.

[2] Unless noted otherwise, residues are numbered according to the sequence for the enzyme from yeast.

10.1021/bi700409b CCC: $37.00
Published on Web 04/20/2007

Scheme 1

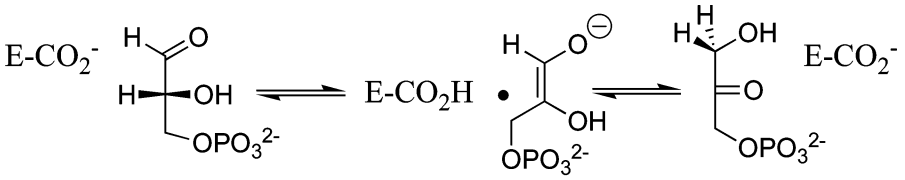

GAP **DHAP**

mutagenesis (*46*−*51*), computational (*52*−*56*), and dynamical approaches (*52*, *57*−*59*).

The binding of phosphodianion ligands to TIM results in a large ca. 7 Å motion of the mobile loop which acts as a "lid" to cover the bound ligand in the active site (*34*, *36*−*38*, *40*−*42*, *44*, *56*, *57*, *59*). The closing of this loop leads to formation of an important hydrogen bond between the backbone amide NH group of Gly-171 at the tip of the mobile loop and a peripheral oxygen of the bound phosphodianion group (*36*, *38*−*40*, *42*, *44*, *45*). The anionic oxygens of the phosphodianion group also interact with the protein via direct hydrogen bonds with backbone amide NH groups in the phosphate binding motif located in loops 7 and 8, and via a water molecule with the essential (*31*) positively charged Lys-12 in the active site (*37*, *40*, *42*, *44*, *60*). Loop closure results in the exclusion of bulk solvent from the active site (*36*−*38*, *40*, *42*) and serves to protect the reactive enediolate intermediate from bulk solution where it undergoes rapid nonenzymatic elimination to give methylglyoxal (*46*, *61*). Despite these well-documented conserved interactions of the protein with the phosphodianion group of bound ligands, there is no consensus about the physical mechanism by which they may be harnessed to stabilize the transition state for proton transfer.

We showed previously (*62*) that deprotonation of the neutral triose sugar (*R*)-glyceraldehyde by TIM is ca. 10^8-fold slower than the partly diffusion-controlled (*11*) turnover of the natural phosphorylated substrate GAP and that more than 80% of the 4×10^{10}-fold enzymatic rate acceleration of proton transfer (*61*, *62*) can be attributed to the presence of the small nonreacting phosphodianion group of the substrate.

Utilization of the binding energy of the substrate phosphodianion group for stabilization of the ground state Michaelis complex with the bound substrate is important, but uninteresting with respect to a rationalization of the enzymatic rate acceleration for TIM. Our earlier data demand that the intrinsic binding energy of the phosphodianion group of GAP be utilized specifically for stabilization of the transition state for proton transfer from carbon. However, this conclusion has not gained wide acceptance, perhaps as a result of the complexity of the experimental evidence that supports it. The goal of this work was to provide simple and more compelling evidence that a portion of the intrinsic binding energy of the substrate phosphodianion group is expressed only on moving from the Michaelis complex to the transition state for deprotonation of GAP by TIM. The demonstration that the interactions of TIM with the phosphodianion group are "catalytic" in the absence of a covalent connection between the phosphodianion and carbon acid portions of GAP would be unequivocal evidence that the oxydianion is not simply an "anchor" for fixing the carbon acid at the active site. This would correspond to an "allosteric" activation of TIM by the separately bound phosphodianion moiety of a truncated substrate.

We report here that the slow deprotonation of the minimal two-carbon neutral substrate glycolaldehyde (*h*-GLY) by TIM in D_2O, which results in formation of monodeuteriated glycolaldehyde (*d*-GLY), can be monitored by ^1H NMR spectroscopy (Scheme 2). The separate binding of exogenous phosphite dianion to TIM results in a very large 700-fold increase in the second-order rate constant for turnover of *h*-GLY. The results strongly support a physical model for catalysis by TIM in which the intrinsic binding energy of the substrate phosphodianion group is utilized to drive closing of the mobile loop and a protein conformational change that leads to formation of an active site environment that is optimally organized for stabilization of the transition state. They suggest that a substantial portion of the rate acceleration for TIM results directly from utilization of the intrinsic binding energy of the remote nonreacting substrate phosphodianion group to lower the kinetic barrier to proton transfer from α-carbonyl carbon.

Scheme 2

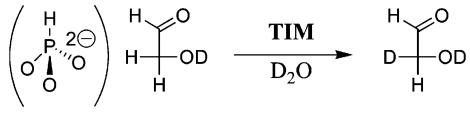

***h*-GLY** ***d*-GLY**

MATERIALS AND METHODS

Triosephosphate isomerase from rabbit muscle (lyophilized powder) was from Sigma and had a specific activity toward GAP of 5500−6000 units/mg at pH 7.5 and 25 °C. Glycerol 3-phosphate dehydrogenase (GPDH) from rabbit muscle was from Roche or MP Biomedicals. Bovine serum albumin (Fraction V, BSA) was from Life Technologies. Glycolaldehyde dimer, triethanolamine hydrochloride, imidazole, sodium phosphate (tribasic), and tetramethylammonium hydrogensulfate were from Aldrich. NADH (disodium salt), D,L-glyceraldehyde 3-phosphate diethyl acetal (barium salt), phosphoglycolic acid [tri(monocyclohexyl)ammonium salt], and Dowex 50WX4-200R were from Sigma. Sodium phosphite (dibasic, pentahydrate) was from Riedel-de Haën (Fluka). Deuterium oxide (99.9% D) and deuterium chloride (35% w/w, 99.9% D) were from Cambridge Isotope Laboratories. Imidazole was recrystallized from benzene. All other chemicals were reagent grade or better and were used without further purification.

Preparation of Solutions. Stock solutions of D,L-glyceraldehyde 3-phosphate (D,L-GAP) at pH 7.4 or 7.5 were prepared by hydrolysis of the diethyl acetal using Dowex 50WX4-200R (H^+ form) followed by neutralization with 1

M NaOH. The concentration of GAP in these solutions was determined via a coupled enzymatic assay, as described previously (*25*).

Triethanolamine buffers (pH 7.5) were prepared by neutralization of the hydrochloride with 1 M NaOH. Buffered solutions of imidazole (50 mM, 70% free base, pH 7.4), phosphite (70 mM, 90% free base), and phosphate (60 mM, 85% free base) for use in competitive inhibition studies were prepared by addition of measured amounts of 1 M HCl to the basic form or the sodium salt.

Buffered solutions of imidazole (30 mM, 20% free base) at pD 7.0 were prepared by dissolving the basic form, and where appropriate NaCl, in D_2O followed by addition of 0.8 equiv of DCl to give the required acid:base ratio at $I = 0.024$ or 0.10.

Before preparation of solutions in D_2O, $Na_2HPO_3{\cdot}5H_2O$ was dried under vacuum at 25 °C for 16 h. Gravimetric analysis and titration showed that this resulted in the loss of 4.6 equiv of H_2O, which corresponds to ca. 40% of the initial weight. The resulting salt ($Na_2HPO_3{\cdot}0.4H_2O$) was stored in a desiccator. Stock solutions of phosphite (40 or 80 mM, $I = 0.10$ or 0.20, respectively) at pD 7.0 were prepared by dissolving $Na_2HPO_3{\cdot}0.4H_2O$ in D_2O followed by addition of 0.5 equiv of DCl to give a 1:1 dianion:monoanion ratio.

A stock solution of phosphate (60 mM, $I = 0.21$) at pD 7.1 was prepared by dissolving sodium phosphate trianion in D_2O followed by addition of 1.5 equiv of DCl to give a 1:1 dianion:monoanion ratio.

Sodium phosphoglycolate tri(monocyclohexyl)ammonium salt in D_2O at pD 6.9 (100 mM, 1:1 trianion:dianion ratio, prepared by addition of 0.5 equiv of DCl) was freed of monocyclohexylamine by being passed down a short column of Dowex 50WX4-200R (D^+ form) that had been equilibrated with D_2O. The acidic fractions were combined, and the concentration of 2-phosphoglycolic acid in the resulting solution (41 mM) was determined by ^{1}H NMR by quantitative integration of the signal due to the methylene group of 2-phosphoglycolate relative to that for the C(4,5)-protons of imidazole buffer that was added as an internal standard. The acidic solution of 2-phosphoglycolic acid (pD ≈1.4) was neutralized by the addition of 3 equiv of concentrated NaOD to give a stock solution of 39 mM 2-phosphoglycolate (PGA) at pD 6.9 (ca. 1:1 trianion:dianion ratio, $I \approx 0.2$, NaCl).

Stock solutions of glycolaldehyde (100 mM) in D_2O at an ionic strength of 0 or 0.10 were prepared by dissolving glycolaldehyde dimer, and where appropriate NaCl, in D_2O and were stored at room temperature to minimize the dimer content. ^{1}H NMR analysis showed that there was negligible dimeric glycolaldehyde present after a 5-fold dilution of this stock solution into 0.1 M NaCl in D_2O (*63*, *64*).

Commercial rabbit muscle TIM (10−16 mg/mL protein) was dialyzed at 4 °C against 30 mM imidazole buffer (20% free base) in D_2O at pD 7.0 and $I = 0.024$ for reactions in the presence of added phosphite or phosphate dianions or $I = 0.10$ (NaCl) for reactions in their absence.

Determination of pL and the pK_a of Phosphite and Phosphate Dianions in D_2O. The solution pH or pD was determined at 25 °C using an Orion model 720A pH meter equipped with a Radiometer pHC4006-9 combination electrode that was standardized at pH 4.00 and 7.00 at 25 °C. Values of pD were obtained by adding 0.40 to the observed reading of the pH meter (*65*). An apparent value of pK_a = 6.99 for ionization of phosphite monoanion in D_2O at 25 °C and $I = 0.10$ (NaCl) was determined as the pD of a solution of 40 mM sodium phosphite at a 1:1 monoanion:dianion ratio. An apparent value of pK_a = 7.22 for ionization of phosphate monoanion in D_2O at 25 °C and $I = 0.10$ (NaCl) was determined as the pD of a solution of 30 mM sodium phosphate at a 1:1 monoanion:dianion ratio.

Enzyme Assays. Enzyme assays were carried out at 25 °C. Changes in the concentration of NADH were calculated from the changes in the absorbance at 340 nm using an extinction coefficient of 6220 M^{-1} cm^{-1}. GPDH was dialyzed at 4 °C against 20 mM triethanolamine buffer (pH 7.5) and was assayed by monitoring the oxidation of NADH by DHAP, as described previously (*25*).

The activity of TIM in the reaction mixtures in D_2O that were monitored by ^{1}H NMR (10−80 units/μL) was determined in standard assays in which the isomerization of GAP was coupled to the oxidation of NADH using GPDH (*20*). Assay mixtures (1.0 mL) contained 100 mM triethanolamine (pH 7.5, $I = 0.1$), 0.2 mM NADH, ca. 6 mM D,L-GAP (3 mM GAP, ∼7K_m), 0.3−0.5 unit of GPDH (3−5 μg), and 5 μL of the reaction mixture after its 10000- or 50000-fold dilution into 20 mM triethanolamine (pH 7.5). Before addition of the reaction mixture containing TIM, the background velocity due mainly to the isomerization of GAP catalyzed by TIM present as a contaminant in the GPDH, v_o, was determined over 2−4 min. This background velocity generally represented ≤3% of the total initial velocity, v_i, that was determined over 5−10 min after the addition of the diluted reaction mixture containing TIM. Values of V_{max} (M s^{-1}) were calculated from the values of $v_i - v_o$ using $K_m = 0.45$ mM for GAP (*20*, *62*). The concentration of TIM in the assay mixture was calculated from the values of V_{max} (M s^{-1}) using the relationship $[TIM]_{assay} = V_{max}/k_{cat}$ with k_{cat} = 4300 s^{-1} (*19*, *66*).

Values of K_i for competitive inhibition of TIM by phosphite and phosphate dianions in H_2O at pH 7.4 and I = 0.12 (NaCl) were determined from the effect of added 35 mM phosphite buffer (90% free base, 31.5 mM dianion) or 27 mM phosphate buffer (85% free base, 23 mM dianion) on the apparent value of K_m for GAP determined in 10 mM imidazole buffer (70% free base) at pH 7.4, 25 °C, and I = 0.12 (NaCl). For these studies, the stock solution of TIM (ca. 0.2 μg/mL) was stabilized by the inclusion of BSA (100 μg/mL) and the amount of GPDH in the coupled assays was increased to 1−2 units (10−20 μg).

Background Reactions of Glycolaldehyde in D_2O Buffered by Imidazole, Phosphite, and Phosphate Followed by ^{1}H NMR. The reactions of glycolaldehyde (19 mM) in D_2O buffered by 24 mM imidazole (20% free base, pD 7.0), 32 mM phosphite (50% free base, pD 7.0), or 30 mM phosphate (50% free base, pD 7.2) at 25 °C and $I = 0.10$ (NaCl) were followed by ^{1}H NMR spectroscopy. Two identical reaction mixtures (1 mL) were prepared by addition of an aliquot of 100 mM glycolaldehyde in D_2O ($I = 0.10$, NaCl) to the buffer. For the reaction in phosphite buffer, the reaction mixture also contained ca. 1 mM tetramethylammonium hydrogensulfate as an internal standard. For the reaction in phosphate buffer, the reaction mixture also contained 6 mM imidazole buffer (pD 7.0). 750 μL of the first reaction

mixture was transferred to a NMR tube, and the NMR spectrum was recorded within 1 h, after which the NMR tube was incubated at 25 °C. The second reaction mixture was incubated at 25 °C and was used to monitor any change in pD during these slow reactions. The reaction in the presence of imidazole was followed for 35 days (19% disappearance of glycolaldehyde, ca. 0.2 unit decrease in pD). The reaction in the presence of phosphite was followed for 39 days (48% reaction, ca. 0.4 unit decrease in pD). The reaction in the presence of phosphate was followed for 13 days (40% reaction, 0.1 unit decrease in pD).

Turnover of Glycolaldehyde by TIM in D_2O in the Absence and Presence of 2-Phosphoglycolate Followed by ^1H NMR. The turnover of glycolaldehyde (19 mM) by TIM in D_2O in the presence of 24 mM imidazole buffer (20% free base, pD 7.0) at 25 °C and $I = 0.10$ (NaCl) was followed by ^1H NMR spectroscopy. The reaction in a volume of 850 μL was initiated by the addition of an aliquot (170 μL) of 100 mM glycolaldehyde in D_2O ($I = 0.10$, NaCl) to a solution of TIM (ca. 100 units/μL, 10 mg/mL) in 30 mM imidazole buffer at pD 7.0 in D_2O ($I = 0.10$, NaCl). 780 μL of the reaction mixture was transferred to a NMR tube, and the NMR spectrum was recorded immediately, after which the NMR tube was incubated at 25 °C. The remainder was incubated at 25 °C, and the activity of TIM in the reaction mixture was determined via a periodic standard assay (see above). The reaction was followed for 38 h, during which time there was 68% reaction of glycolaldehyde and no significant decrease in enzyme activity (±10%). The solution was then removed from the NMR tube, and 163 μL of a solution of PGA at pD 7.0 in D_2O (39 mM, $I = 0.20$, prepared as described above) was added to 650 μL of the recovered reaction mixture. This gave a new reaction mixture containing ca. 5 mM unreacted glycolaldehyde, 7.8 mM PGA, and 19 mM imidazole in D_2O ($I = 0.12$). 750 μL of this solution was transferred to a NMR tube, and the NMR spectrum was recorded immediately, after which the NMR tube was incubated at 25 °C. The remainder was incubated at 25 °C, and the activity of TIM was determined via a periodic standard assay (see above). The reaction that included PGA was followed for 5 days, during which time there was 68% reaction of the remaining glycolaldehyde and no significant decrease in enzyme activity (±10%). After 7 days, the solution was removed from the NMR tube, the protein was removed by ultrafiltration using an Amicon Microcon device (10 000 MWCO), and the pD of the filtrate was determined. This showed that there was only a small 0.15 unit decrease in the pD of the reaction mixture during the total reaction time of 9 days.

Turnover of Glycolaldehyde by TIM in D_2O in the Presence of Phosphite and Phosphate Dianions Followed by ^1H NMR. The turnover of glycolaldehyde by TIM in D_2O in the presence of 4.9−40 mM phosphite buffer (50% dianion, pD 7.0) or 30 mM phosphate buffer (50% dianion, pD 7.2) at 25 °C and $I = 0.10$ (NaCl) was followed by ^1H NMR spectroscopy. Reactions in a volume of 750 μL were initiated by addition of 150 μL of a solution of TIM (ca. 60 units/μL, 6 mg/mL) in 30 mM imidazole buffer at pD 7.0 in D_2O ($I = 0.024$) to the reaction mixture containing glycolaldehyde, phosphite or phosphate buffer, and NaCl in D_2O to give final concentrations of 19 or 9.5 mM glycolaldehyde, 6 mM imidazole, and 2.5−20 mM inorganic oxydianion at $I = 0.10$ (NaCl). 700 μL of the reaction mixture was transferred to a NMR tube, and the NMR spectrum was recorded immediately. The remainder was incubated at 25 °C, and the activity of TIM was determined via a periodic standard assay (see above). For the reactions in the presence of phosphite, the NMR tube was left in the probe at 25 °C and spectra (8−16 transients) were recorded at 12−24 min intervals for up to 13 h. The reaction in the presence of phosphate was followed for 6 days. In several cases, the solution was removed from the NMR tube at the end of the reaction, the protein was removed by ultrafiltration using an Amicon Microcon device (10 000 MWCO), and the pD of the filtrate was determined. This showed that there was no significant change in pD during the turnover of glycolaldehyde by TIM in these experiments.

^1H NMR Analyses. ^1H NMR spectra at 500 MHz were recorded in D_2O at 25 °C using a Varian Unity Inova 500 spectrometer that was shimmed to give a line width of ≤0.4 Hz for the downfield peak of the triplet due to the C-1 proton of glycolaldehyde hydrate. The probe temperature was determined from the difference in the chemical shifts of the hydroxyl and methyl protons of methanol containing a trace of HCl (*67*). Spectra (8−32 transients) were obtained using a sweep width of 6000 Hz, a pulse angle of 90°, and acquisition times of 6−9 s, with zero-filling of the data to 128 K. To ensure accurate integrals for the protons of interest, a relaxation delay between pulses of 90−120 s ($>8T_1$) was used (see below). Baselines were subjected to a first-order drift correction before determination of integrated peak areas. Chemical shifts are reported relative to HOD at 4.67 ppm.

The following relaxation times (T_1) were determined in D_2O at 25 °C and $I = 0.10$ (NaCl). (a) The protons of glycolaldehyde hydrate (19 mM) in 24 mM imidazole buffer at pD 7.0: $T_1 = 11$ s (C1-proton) and 3 s (C2-protons). (b) The protons of the free carbonyl form of glycolaldehyde (19 mM) in 32 mM phosphite buffer at pD 7.0: $T_1 = 14$ s (C1-proton) and 6 s (C2-protons). (c) The C(4,5)-protons of imidazole (24 mM) at pD 7.0: $T_1 = 15$ s. (d) The P-H proton of phosphite (32 mM) at pD 7.0: $T_1 = 5$ s.

Integrated peak areas were normalized to that of an appropriate internal standard. For the background reactions in imidazole buffer and in phosphate buffer containing imidazole, the internal standard was the signal at 7.3 ppm due to the C(4,5)-protons of imidazole. For the background reaction in phosphite buffer, the internal standard was the triplet at 3.1 ppm due to the methyl groups of added tetramethylammonium hydrogensulfate. For the TIM-catalyzed reactions in the presence of phosphite, the internal standard was the upfield peak of the doublet at 6.7 ppm ($J = 600$ Hz) due to the P-H proton of phosphite. For the TIM-catalyzed reactions in the absence of phosphite, the internal standard was the signal at 7.3 ppm due to the C(4,5)-protons of imidazole.

The integrated area of the signal due to the C1-proton of *h*-GLY hydrate was evaluated using eq 1

$$A_{h-\mathrm{GLY}} = 4a \qquad (1)$$

where a is the area of the downfield peak of the triplet due to the C1-proton of *h*-GLY hydrate. The integrated area of

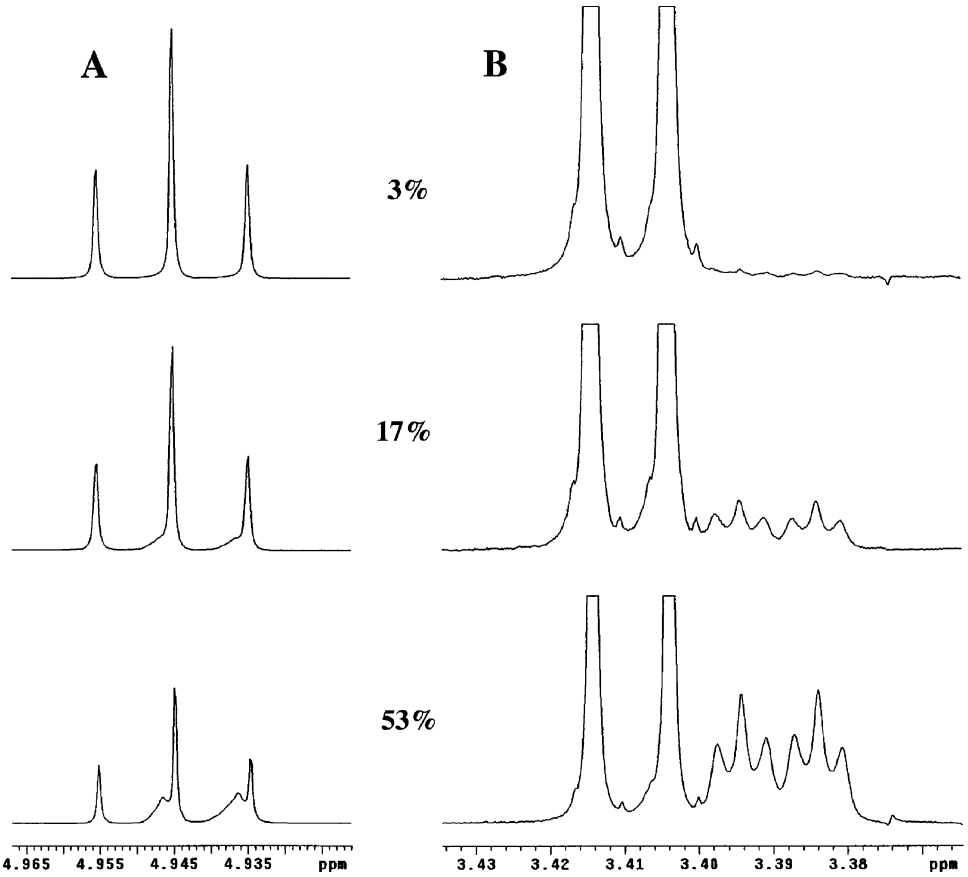

FIGURE 1: Partial ^{1}H NMR spectra at 500 MHz obtained at various times during the reaction of 19 mM *h*-GLY in the presence of 0.31 mM (8.3 mg/mL) rabbit muscle TIM and 24 mM imidazole buffer (pD 7.0) in D_2O at 25 °C ($I = 0.10$). The extent of reaction of *h*-GLY is given above each spectrum. (A) The turnover of *h*-GLY results in the disappearance of the triplet at 4.945 ppm ($J = 5$ Hz) due to the C1-proton of *h*-GLY hydrate and the appearance of a broad upfield-shifted doublet at 4.942 ppm ($\Delta\delta = 0.003$ ppm; $J = 5$ Hz) due to the C1-proton of the hydrate of glycolaldehyde labeled with deuterium at C2 (*d*-GLY). At late reaction times, the upfield peak of this doublet appears larger than the downfield peak as a result of the formation of the hydrate of glycolaldehyde labeled with two deuteriums at C2, which exhibits a broad singlet at 4.936 ppm. (B) The turnover of *h*-GLY results in the disappearance of the doublet at 3.409 ppm ($J = 5$ Hz) due to the two C2-protons of *h*-GLY hydrate and the appearance of an upfield-shifted double triplet at 3.389 ppm ($\Delta\delta = 0.02$ ppm) due to the single C2-proton of *d*-GLY hydrate. This proton is coupled to both the C1-proton ($J = 5$ Hz) and the geminal deuterium ($J = 1.6$ Hz).

the signal due to the C1-proton of *d*-GLY hydrate was evaluated using eq 2

$$A_{d-\mathrm{GLY}} = 2b - 4a \tag{2}$$

where *b* is the sum of the areas of the downfield peak of the doublet due to the C1-proton of *d*-GLY hydrate and the center peak of the triplet due to the C1-proton of *h*-GLY hydrate (see Figure 1).

The fractions of *h*-GLY and *d*-GLY present at time *t* were calculated according to eqs 3 and 4

$$f_{h-\mathrm{GLY}} = \frac{A_{h-\mathrm{GLY}}}{(A_{h-\mathrm{GLY}})_o + (A_{d-\mathrm{GLY}})_o} \tag{3}$$

$$f_{d-\mathrm{GLY}} = \frac{A_{d-\mathrm{GLY}}}{(A_{h-\mathrm{GLY}})_o + (A_{d-\mathrm{GLY}})_o} \tag{4}$$

where $(A_{h-\mathrm{GLY}})_o$ and $(A_{d-\mathrm{GLY}})_o$ are the integrated areas of the signals due to the C1-protons of the hydrates of *h*-GLY and *d*-GLY, respectively, obtained from the first NMR spectrum, for which *t* was defined as zero. This analysis neglects the small amounts (≤3%) of dideuteriated glycolaldehyde that are already formed at time zero in the relatively fast TIM-catalyzed reactions in the presence of phosphite dianion. The *total* concentration of glycolaldehyde present in the reaction mixture was obtained by comparison of the value of $(A_{h-\mathrm{GLY}})_o + (A_{d-\mathrm{GLY}})_o$ with the integrated area of the signal due to the C(4,5)-protons of imidazole, or that of the upfield peak of the doublet due to the P-H proton of phosphite, with a correction for the presence of 6.1% of the free carbonyl form of glycolaldehyde. For the slow background reactions in the absence of TIM, there was no detectable formation of *d*-GLY at time zero so that $(A_{d-\mathrm{GLY}})_o = 0$.

Observed first-order rate constants k_{obsd} (s^{-1}) for the disappearance of *h*-GLY were determined from the slopes of linear semilogarithmic plots of reaction progress against time according to eq 5

$$\ln[f_{h-\mathrm{GLY}}/(f_{h-\mathrm{GLY}})_o] = -k_{obsd}t \tag{5}$$

where $(f_{h-\mathrm{GLY}})_o$ is the fraction of *h*-GLY present in the reaction mixture at time zero. For the slow background reactions in buffered D_2O, $(f_{h-\mathrm{GLY}})_o = 1.0$ and these plots covered up to ca. 50% disappearance of the starting *h*-GLY. For the TIM-catalyzed reactions, $(f_{h-\mathrm{GLY}})_o \geq 0.8$ and these plots covered disappearance of 60−80% of the starting *h*-GLY.

RESULTS

Quantitative integration of the triplet at 4.95 ppm due to the C1-proton of glycolaldehyde hydrate and the singlet at 4.34 ppm due to the C2-protons of the free carbonyl form of glycolaldehyde in the ^{1}H NMR spectrum of 19 mM glycolaldehyde in 32 mM phosphite buffer (50% free base, pD 7.0) showed that glycolaldehyde exists as 93.9% hydrate and 6.1% free carbonyl form in D_2O at 25 °C and $I = 0.10$ (NaCl). This gives $K_{hyd} = 15.4$ as the equilibrium constant for hydration of the carbonyl group of glycolaldehyde under these conditions (Scheme 3). This is similar to the values of $K_{hyd} \approx 17.5$ calculated from NMR data for 0.1 M glycolaldehyde in D_2O at 35 °C (*63*) and $K_{hyd} = 18.0 \pm 3.3$ in D_2O at 25 °C determined by NMR (*64*). In the presence of imidazole buffer (≥6 mM) at pD 7.0 and 25 °C, the ^{1}H NMR signals due to the free carbonyl form of glycolaldehyde are severely exchange broadened or not observed, as a result of formation of the adduct of imidazole to the carbonyl group. The ^{1}H NMR spectrum of 19 mM glycolaldehyde in 0.8 M imidazole buffer (70% free base, pD 7.9) at 25 °C and $I = 0.3$ (NaCl) exhibits signals due to glycolaldehyde hydrate at 4.86 ppm (triplet, C1H) and 3.32 ppm (doublet, C2H), along with signals assigned to an approximately equal amount of the corresponding imidazole adduct at ca. 5.7 ppm (very broad, C1H) and 3.71 ppm (broad, C2H) (data not shown).

Scheme 3

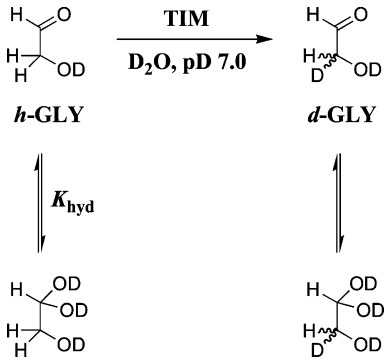

Figure 1 shows partial ^{1}H NMR spectra at 500 MHz obtained at various times during the reaction of 19 mM glycolaldehyde (*h*-GLY) in the presence of 0.31 mM (8.3 mg/mL) rabbit muscle triosephosphate isomerase (TIM) and 24 mM imidazole buffer (pD 7.0) in D_2O at 25 °C and $I = 0.10$ (NaCl). The slow turnover of *h*-GLY by TIM results in the disappearance of the triplet at 4.945 ppm ($J = 5$ Hz) due to the C1-proton of *h*-GLY hydrate and the appearance of a broad upfield-shifted doublet at 4.942 ppm ($\Delta\delta = 0.003$ ppm, $J = 5$ Hz) due to the C1-proton of the hydrate of glycolaldehyde labeled with deuterium at C2 [*d*-GLY (Scheme 3)]. At late reaction times, the upfield peak of this doublet appears larger than the downfield peak as a result of the formation of glycolaldehyde hydrate labeled with two deuteriums at C2, which exhibits a broad singlet at 4.936 ppm. Similarly, disappearance of the doublet at 3.409 ppm ($J = 5$ Hz) due to the two C2-protons of *h*-GLY hydrate is accompanied by the appearance of an upfield-shifted double triplet at 3.389 ppm ($\Delta\delta = 0.02$ ppm) due to the single C2-proton of the first-formed *d*-GLY hydrate product, which is coupled to both the C1-proton ($J = 5$ Hz) and the geminal deuterium ($J = 1.6$ Hz) (Scheme 3). The magnitude of these deuterium isotope effects on ^{1}H chemical shifts and the geminal H−D coupling constant are similar to those observed in our earlier work for incorporation of deuterium into GAP (*25*), DHAP (*25*), dihydroxyacetone (*68*, *69*), and hydroxyacetone (*70*).

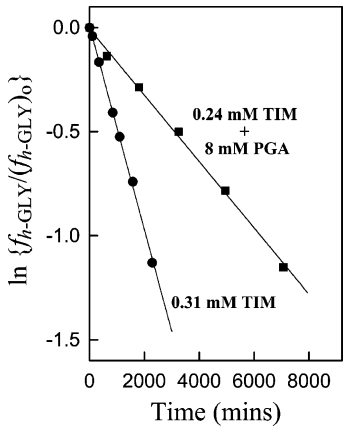

FIGURE 2: Semilogarithmic time courses for the reaction of *h*-GLY in D_2O at pD 7.0 and 25 °C catalyzed by rabbit muscle TIM, followed by ^{1}H NMR spectroscopy by monitoring the decrease in the area of the downfield peak of the triplet due to the C1-proton of *h*-GLY hydrate: (●)19 mM *h*-GLY in the presence of 0.31 mM TIM and 24 mM imidazole buffer ($I = 0.10$) and (■) 5 mM *h*-GLY in the presence of 0.24 mM TIM, 19 mM imidazole buffer, and 8 mM PGA ($I = 0.12$).

Figure 2 (●) shows the semilogarithmic time course for the disappearance of 68% of 19 mM *h*-GLY in the presence of 0.31 mM (8.3 mg/mL) rabbit muscle TIM and 24 mM imidazole buffer (pD 7.0) in D_2O at 25 °C and $I = 0.10$ (NaCl), followed by ^{1}H NMR spectroscopy by monitoring the decrease in the area of the downfield peak of the triplet due to the C1-proton of *h*-GLY hydrate (Figure 1A). The data give $k_{obsd} = 8.2 \times 10^{-6}$ s^{-1} as the first-order rate constant for the disappearance of *h*-GLY, which is 120-fold larger than $k_o = 7.0 \times 10^{-8}$ s^{-1} determined for the disappearance of *h*-GLY in the absence of TIM under the same conditions (see below). Therefore, essentially all of the reaction of *h*-GLY can be attributed to the presence of the protein catalyst with $k_{obsd} = 8.1 \times 10^{-6}$ s^{-1} for turnover of *h*-GLY by TIM in this experiment.

Figure 2 (■) shows the semilogarithmic time course for the disappearance of 68% of 5 mM *h*-GLY in the presence of 0.24 mM (6.4 mg/mL) rabbit muscle TIM, 19 mM imidazole buffer (pD 7.0), and 8 mM of the potent competitive inhibitor 2-phosphoglycolate [PGA; $K_i \approx 5$ μM at pH 7.0 and $I = 0.1$ (*22*)] in D_2O at 25 °C and $I = 0.12$ (NaCl), followed by ^{1}H NMR spectroscopy. The data give $k_{obsd} = 2.7 \times 10^{-6}$ s^{-1} as the first-order rate constant for the disappearance of *h*-GLY, which is 22-fold larger than $k_{obsd} \approx 1.2 \times 10^{-7}$ s^{-1} estimated[3] for the disappearance of *h*-GLY in the absence of TIM under the same conditions. This gives $k_{obsd} = 2.6 \times 10^{-6}$ s^{-1} for the nonspecific protein-catalyzed disappearance of *h*-GLY in the presence of a saturating amount of PGA in this experiment (*62*).

[3] Estimated from $k_{obsd} = 7.0 \times 10^{-8}$ s^{-1} for the disappearance of glycolaldehyde in the presence of 24 mM imidazole buffer at pD 7.0 (this work) and the 1.8-fold higher reactivity of glyceraldehyde in 18 mM imidazole buffer containing 8 mM PGA at pD 7.0 than in the presence of 24 mM imidazole buffer at pD 7.0 (see ref *63*).

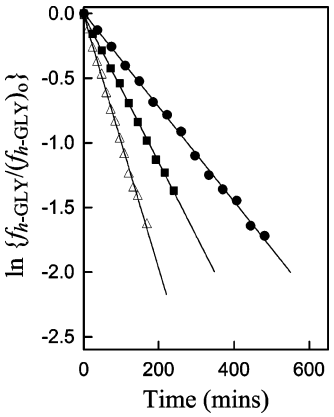

FIGURE 3: Representative semilogarithmic time courses for the reaction of 19 mM *h*-GLY catalyzed by 42 μM rabbit muscle TIM in the presence of phosphite dianion and 6 mM imidazole in D_2O at pD 7.0 and 25 °C ($I = 0.10$), followed by ^{1}H NMR spectroscopy by monitoring the decrease in the area of the downfield peak of the triplet due to the C1-proton of *h*-GLY hydrate. Key: (●) $[HPO_3^{2-}] = 5$ mM; (■) $[HPO_3^{2-}] = 10$ mM; (△) $[HPO_3^{2-}] = 20$ mM.

Observed first-order rate constants for the slow nonenzymatic background reactions of 19 mM *h*-GLY in buffered D_2O at 25 °C and $I = 0.10$ (NaCl) were determined by ^{1}H NMR spectroscopy by monitoring the decrease in the area of the downfield peak of the triplet due to the C1-proton of *h*-GLY hydrate (Figure 1A). The data give $k_o = 7.0 \times 10^{-8}$ s^{-1} for the reaction in the presence of 24 mM imidazole buffer (20% free base, pD 7.0) determined during the disappearance of 19% *h*-GLY, $k_o = 2.4 \times 10^{-7}$ s^{-1} for the reaction in the presence of 32 mM phosphite buffer (50% free base, pD 7.0) determined during the disappearance of 48% of *h*-GLY, and $k_o = 4.3 \times 10^{-7}$ s^{-1} for the reaction in the presence of 30 mM phosphate buffer (50% free base, pD 7.2) containing 6 mM imidazole determined during the disappearance of 40% of *h*-GLY.

Figure 3 shows representative semilogarithmic time courses for the disappearance of 19 mM *h*-GLY catalyzed by 42 μM rabbit muscle TIM in the presence of various concentrations of phosphite dianion and 6 mM imidazole in D_2O at pD 7.0 and 25 °C ($I = 0.10$, NaCl). Table 1 summarizes the observed first-order rate constants k_{obsd} (s^{-1}) determined for the reaction of 19 or 9.5 mM *h*-GLY in experiments conducted in the presence of 2.5−20 mM phosphite dianion.

A value of $k_{obsd} = 3.3 \times 10^{-6}$ s^{-1} was determined for the reaction of 19 mM *h*-GLY in the presence of 42 μM rabbit muscle TIM, 6 mM imidazole, and 30 mM phosphate buffer (50% free base, pD 7.2). This is only 7.7-fold faster than $k_o = 4.3 \times 10^{-7}$ s^{-1} determined for the reaction in the absence of TIM under the same conditions (see above). The net rate constant for turnover of *h*-GLY by 42 μM TIM in the presence of 15 mM phosphate dianion at pD 7.2 is therefore $k_{obsd} = 2.9 \times 10^{-6}$ s^{-1}.

The Michaelis constant for turnover of GAP (0.07−3.6 mM) by rabbit muscle TIM in 10 mM imidazole buffer in H_2O at pH 7.4, 25 °C, and $I = 0.12$ (NaCl) was determined as $K_m = 0.50$ mM. This is comparable with $K_m = 0.45$ mM determined in 0.1 M triethanolamine buffer at pH 7.5, 25 °C, and $I = 0.1$ (*62*). The addition of 35 mM phosphite buffer (31.5 mM dianion) resulted in competitive inhibition and a value of $(K_m)_{app} = 1.04$ mM, which can be combined with $K_m = 0.50$ mM to give $K_i = 29$ mM for binding of phosphite dianion to TIM in H_2O at pH 7.4 and $I = 0.12$. There was no detectable change in the value of $(K_m)_{app}$ for GAP under these conditions upon addition of 20 mM glycolaldehyde. Similarly, the addition of 27 mM phosphate buffer (23.0 mM dianion) resulted in competitive inhibition and a value of $(K_m)_{app} = 1.40$ mM, which gives $K_i = 13$ mM for binding of phosphate dianion to TIM in H_2O at pH 7.4 and $I = 0.12$. This is consistent with $K_i \approx 5$ mM for phosphate determined at pH 7.7 and low ionic strength (*71*) and the marked effect of ionic strength on the affinity of TIM for phosphodianion ligands (*22*).

Table 1: Rate Constants for the Turnover of Glycolaldehyde (*h*-GLY) To Give Monodeuteriated Glycolaldehyde (*d*-GLY) by 42 μM Triosephosphate Isomerase in the Presence of Various Concentrations of Phosphite Dianion and 6 mM Imidazole in D_2O at pD 7.0 and 25 °C ($I = 0.10$, NaCl)

$[HPO_3^{2-}]^a$ (mM)	$[GLY]_{tot}^b$ (mM)	k_{obsd}^c (s^{-1})	k_{TIM}^d (M^{-1} s^{-1})	$(k_{cat}/K_m)_{obsd}^e$ (M^{-1} s^{-1})
0	19		0.0158[f]	0.26
2.5	19	3.60×10^{-5}	0.853	14.0
5.0	19	6.08×10^{-5}	1.44	23.6
10.0	19	9.52×10^{-5}	2.26	37.0
10.0	9.5	9.98×10^{-5}	2.36	38.7
15.0	19	1.32×10^{-4}	3.13	51.3
20.0	19	1.64×10^{-4}	3.89	63.8
20.0	9.5	1.70×10^{-4}	4.03	66.1

[a] Concentration of phosphite dianion added as phosphite buffer (50% free base, pD 7.0). [b] Total concentration of glycolaldehyde. [c] Observed first-order rate constant for the disappearance of *h*-GLY, determined from the slope of a semilogarithmic plot of reaction progress vs time according to eq 5 (see Figure 3). [d] Second-order rate constant for turnover of *h*-GLY by TIM to give *d*-GLY, calculated using the relationship $k_{TIM} = k_{obsd}/[TIM]$, where $[TIM] = 42$ μM, unless noted otherwise. No corrections are made for the background reaction catalyzed by phosphite dianion ($k_o = 2.4 \times 10^{-7}$ s^{-1} in the presence of 32 mM phosphite buffer at pD 7.0) and the nonspecific TIM-catalyzed reaction that occurs outside the active site ($k_{non}[TIM] = 4.5 \times 10^{-7}$ s^{-1}) because they contribute ≤1% to the overall reaction (see the text). [e] Second-order rate constant for turnover of the free carbonyl form of *h*-GLY by TIM, calculated using the relationship $(k_{cat}/K_m)_{obsd} = k_{TIM}(1 + K_{hyd})$, where $K_{hyd} = 15.4$. [f] Second-order rate constant for turnover of glycolaldehyde at the active site of TIM determined in the presence of 24 mM imidazole buffer (pD 7.0).

DISCUSSION

We showed previously (*62*) that the TIM-catalyzed reaction of the neutral triose sugar (*R*)-glyceraldehyde in D_2O gives a complex mixture of products resulting from isomerization to give dihydroxyacetone, isomerization with deuterium exchange to give [1-^{2}H]-dihydroxyacetone, "simple" deuterium exchange to give [2-^{2}H]-glyceraldehyde, and a substantial amount of methylglyoxal from the formal elimination of water (Scheme 4). Moreover, all of these exist as mixtures of free carbonyl and hydrated forms in aqueous solution (*25*, *62*, *64*, *72*, *73*).

Scheme 4

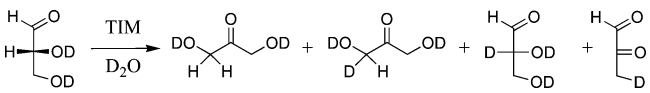

By contrast, isomerization of the minimal two-carbon substrate glycolaldehyde (*h*-GLY) is a degenerate reaction; its isomerization with deuterium exchange and simple

deuterium exchange reactions both give glycolaldehyde labeled with one deuterium at C2 (*d*-GLY), and no elimination reaction is possible (Scheme 5). This greatly simplifies study of the turnover of this neutral substrate by TIM in D_2O because the sole initial product (*d*-GLY) corresponds to that for simple deuterium incorporation, glycolaldehyde exists largely as its hydrate in solution ($K_{hyd} = 15.4$; see Results), and *h*-GLY and *d*-GLY will be hydrated to the same extent.[4]

Scheme 5

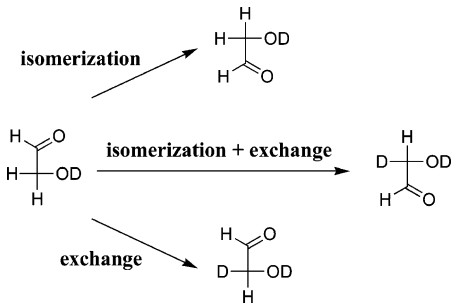

Figure 1 shows that the slow reaction of 19 mM *h*-GLY in the presence of a large amount of TIM (0.31 mM) in D_2O buffered at pD 7.0 can be conveniently monitored by ^1H NMR spectroscopy because there are distinct signals for the hydrates of the substrate *h*-GLY and the first-formed product *d*-GLY in both the C1 and the C2 regions of the spectrum.[5] Good first-order kinetics were observed for this reaction [Figure 2 (●)], and the data give the second-order rate constant for the TIM-catalyzed disappearance of *h*-GLY as $k_{enz} = 8.1 \times 10^{-6}$ s^{-1}/[TIM] = 0.0264 M^{-1} s^{-1}. However, the observation that the presence of a saturating concentration (8 mM) of the potent competitive inhibitor 2-phosphoglycolate [$K_i \approx 5$ μM at pH 7.0 and $I = 0.1$ (*22*)] results in a <3-fold decrease in the observed rate constant for the disappearance of *h*-GLY [Figure 2 (■)] shows that there is a substantial protein-catalyzed reaction of *h*-GLY that occurs *outside the active site*. The second-order rate constant for this nonspecific protein-catalyzed deuterium exchange reaction of *h*-GLY can be calculated as $k_{non} = 2.6 \times 10^{-6}$ s^{-1}/[TIM] = 0.0106 M^{-1} s^{-1}. Therefore, the turnover of *h*-GLY by deprotonation at the active site of TIM with an observed second-order rate constant of $k_{TIM} = 0.0264 - 0.0106 = 0.0158$ M^{-1} s^{-1} is so slow that it is only 1.5-fold faster than its nonspecific protein-catalyzed deuterium exchange reaction.

Similarly, we reported previously that the TIM-catalyzed turnover of (*R*)-glyceraldehyde is only 2-fold faster than its nonspecific protein-catalyzed degradation reaction that occurs outside the active site (*62*). For (*R*)-glyceraldehyde, the nonspecific reaction results mainly in the formation of methylglyoxal, the product of the formal elimination of water. However, for glycolaldehyde, no elimination reaction is possible and the nonspecific reaction results in simple deuterium exchange. The second-order rate constants for the nonspecific protein-catalyzed reactions of glycolaldehyde [0.01 M^{-1} s^{-1} (this work)] and (*R*)-glyceraldehyde [0.009 M^{-1} s^{-1}, calculated from our earlier data (*62*)] are essentially identical. This suggests a common mechanism for these nonspecific reactions, likely involving formation of a Schiff's base adduct between the substrate aldehyde group and lysine residues (*74*, *75*), followed by proton abstraction to give an enzyme-bound iminium ion-stabilized carbanion that undergoes either incorporation of deuterium from solvent to give *d*-GLY or β-elimination to give methylglyoxal.

TIM is specific for the binding and turnover of the free carbonyl forms of its natural substrates DHAP and GAP (*11*), and the true second-order rate constant for turnover of the free carbonyl form of glycolaldehyde (which constitutes 6.1% of the total) at the active site of TIM can be calculated as $(k_{cat}/K_m)_E = 0.0158/0.061 = 0.26$ M^{-1} s^{-1}. This is similar to $k_{cat}/K_m = 0.34$ M^{-1} s^{-1} for turnover of the free carbonyl form of (*R*)-glyceraldehyde by TIM under the same conditions (*62*). Therefore, the truncation of this neutral triose to give the minimal neutral substrate glycolaldehyde has a negligible effect on the ability of TIM to catalyze proton transfer from α-carbonyl carbon. This shows that there is little or no overall contribution of the terminal hydroxymethylene group of (*R*)-glyceraldehyde to the catalytic rate acceleration for TIM and that glycolaldehyde is an appropriate model for the reacting triose sugar portion of the natural substrate GAP.

Activation of TIM by Binding of Exogenous Phosphite Dianion. Figure 3 shows that there is a strong dependence of the observed first-order rate constant for turnover of 19 mM *h*-GLY by 42 μM TIM in D_2O on the concentration of exogenous phosphite dianion at a constant ionic strength of 0.10 (NaCl). The data are summarized in Table 1. The observation of identical values of k_{obsd} for the disappearance of 19 or 9.5 mM glycolaldehyde, corresponding to the free carbonyl form at 1.2 or 0.6 mM, respectively, shows that there is no significant saturation of TIM by glycolaldehyde at these concentrations. This is further supported by the absence of any detectable effect of 20 mM glycolaldehyde on the value of $(K_m)_{app}$ for turnover of GAP by TIM in the presence of 32 mM phosphite dianion at pH 7.4 (see Results).

The values of k_{obsd} (s^{-1}) in Table 1 are at least 100-fold larger than $k_o = 2.4 \times 10^{-7}$ s^{-1} determined for the background reaction of glycolaldehyde in the presence of 32 mM phosphite buffer (50% dianion, pD 7.0) and k_{non}[TIM] = 0.0106 M^{-1} s^{-1} × 42 μM = 4.5×10^{-7} s^{-1} for the nonspecific protein-catalyzed reaction of *h*-GLY catalyzed by 42 μM TIM (see above). Therefore, observed second-order rate constants $(k_{cat}/K_m)_{obsd}$ (M^{-1} s^{-1}) for turnover of the free carbonyl form of *h*-GLY by TIM in the presence of phosphite dianion (Table 1) were calculated directly from the values of $k_{TIM} = k_{obsd}$/[TIM] using the relationship $(k_{cat}/K_m)_{obsd} = k_{TIM}(1 + K_{hyd})$, with $K_{hyd} = 15.4$ determined for hydration of the carbonyl group of glycolaldehyde under the experimental conditions.

Figure 4 shows the dependence of the values of $(k_{cat}/K_m)_{obsd}$ (M^{-1} s^{-1}) for turnover of the free carbonyl form of *h*-GLY by TIM in D_2O on the concentration of exogenous phosphite dianion at pD 7.0 and 25 °C ($I = 0.10$, NaCl). There is a large 250-fold increase in the observed second-order rate constant for turnover of *h*-GLY by TIM upon addition of 20 mM phosphite dianion to the reaction mixture (Table 1),

[4] The secondary deuterium isotope effect on the equilibrium addition of methanol to d_6-acetone to give the hemiketal is $K_H/K_D = 1.29$ (*93*) which corresponds to 4% per β-deuterium. Therefore, the presence of a single β-deuterium will have a negligible effect on the fraction of glycolaldehyde that exists as the hydrate.

[5] The multiple turnover of glycolaldehyde to give dideuteriated glycolaldehyde and other products will be discussed in a future publication.

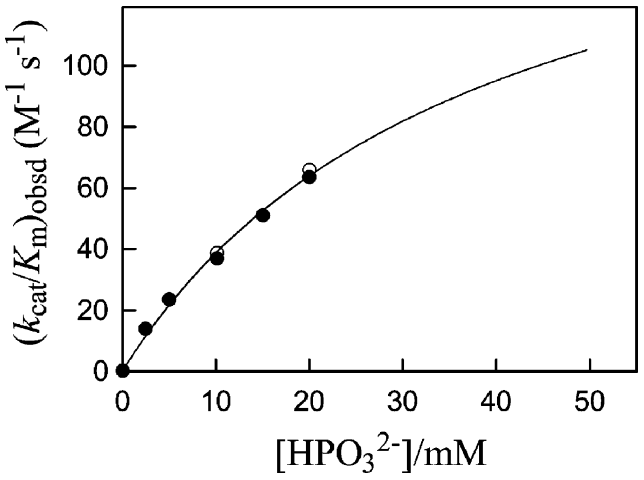

FIGURE 4: Dependence of the observed second-order rate constant $(k_{cat}/K_m)_{obsd}$ (M^{-1} s^{-1}) for turnover of the free carbonyl form of *h*-GLY by TIM in D_2O on the concentration of added phosphite dianion at pD 7.0 and 25 °C ($I = 0.10$). The data were fit to eq 6 to give $K_d = 38 \pm 9$ mM for binding of phosphite dianion to the free enzyme and $(k_{cat}/K_m)_{E\cdot HP_i} = 185 \pm 30$ M^{-1} s^{-1} for turnover of *h*-GLY by TIM that is saturated with phosphite dianion: (●) $[GLY]_{tot} = 19$ mM and (○) $[GLY]_{tot} = 9.5$ mM.

and the dependence of $(k_{cat}/K_m)_{obsd}$ on $[HPO_3^{2-}]$ exhibits saturation (Figure 4). This behavior is consistent with a model in which the binding of phosphite dianion to the free enzyme E gives a noncovalent $E\cdot HPO_3^{2-}$ species that is much more reactive toward proton transfer from glycolaldehyde (S) than is the free enzyme E (Scheme 6).

Scheme 6

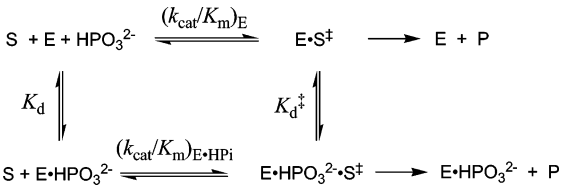

$$(k_{cat}/K_m)_{obsd} = \left(\frac{K_d}{K_d + [HPO_3^{2-}]}\right)(k_{cat}/K_m)_E + \left(\frac{[HPO_3^{2-}]}{K_d + [HPO_3^{2-}]}\right)(k_{cat}/K_m)_{E\cdot HP_i} \quad (6)$$

The data in Table 1 and Figure 4 were fit to eq 6 derived for the model shown in Scheme 6 in which the free enzyme catalyzes proton transfer from *h*-GLY with $(k_{cat}/K_m)_E = 0.26$ M^{-1} s^{-1}, while the binding of phosphite dianion to the free enzyme to give the noncovalent $E\cdot HPO_3^{2-}$ complex results in an enzyme that is much more reactive, with a second-order rate constant $(k_{cat}/K_m)_{E\cdot HP_i}$. This procedure gave $K_d = 38 \pm 9$ mM for binding of phosphite dianion to the free enzyme and $(k_{cat}/K_m)_{E\cdot HP_i} = 185 \pm 30$ M^{-1} s^{-1} as the second-order rate constant for turnover of *h*-GLY by TIM that is saturated with phosphite dianion. Therefore, the separate binding of phosphite dianion to TIM results in a dramatic 700-fold increase in the second-order rate constant for turnover of the minimal truncated substrate glycolaldehyde. The value of $K_d = 38$ mM in D_2O at pD 7.0 and $I = 0.10$ is similar to $K_i = 29$ mM determined for competitive inhibition of the turnover of GAP by phosphite dianion in H_2O at pH 7.4 and $I = 0.12$. This provides further support for the conclusion that the saturation observed in Figure 4 results from the binding of phosphite dianion to the free enzyme.

The thermodynamic cycle shown in Scheme 6 shows that the values of $(k_{cat}/K_m)_E = 0.26$ M^{-1} s^{-1} and $(k_{cat}/K_m)_{E\cdot HP_i} = 185$ M^{-1} s^{-1} can be combined with $K_d = 38$ mM for binding of phosphite dianion to the free enzyme in the ground state to give $K_d^{\ddagger} = 53$ μM as the dissociation constant for phosphite dianion from the fleeting complex of the enzyme with the transition state for deprotonation of *h*-GLY to form the enediolate intermediate, $E\cdot S^{\ddagger}$. Therefore, phosphite dianion binds 700-fold more tightly to the enzyme in the transition state for proton transfer from carbon than it does to the free enzyme in the ground state.

These facts are represented graphically in Figure 5A which relates the free energy profiles for turnover of glycolaldehyde (S) by the free enzyme (E) and by TIM saturated with phosphite dianion ($E\cdot HPO_3^{2-}$). The observed tighter binding of phosphite dianion to the transition state complex $E\cdot S^{\ddagger}$ to give the ternary complex $E\cdot HPO_3^{2-}\cdot S^{\ddagger}$ ($K_d^{\ddagger} = 53$ μM, $\Delta G_o = -5.8$ kcal/mol) than to the free enzyme E ($K_d = 38$ mM, $\Delta G_o = -1.9$ kcal/mol) represents a large "interaction energy" of 3.9 kcal/mol (*76*, *77*). Conversely, it also corresponds to the tighter binding of the altered substrate in the transition state to the binary complex $E\cdot HPO_3^{2-}$ to give the same ternary complex $E\cdot HPO_3^{2-}\cdot S^{\ddagger}$ than to the free enzyme to give $E\cdot S^{\ddagger}$ (Figure 5A). In other words, the free enzyme has LOW affinities for both phosphite dianion ($K_d = 38$ mM) and the altered substrate in the transition state [represented by $(k_{cat}/K_m)_E = 0.26$ M^{-1} s^{-1}], but its binary complexes have HIGH affinities for phosphite dianion ($K_d^{\ddagger} = 53$ μM) and the altered substrate in the transition state [represented by $(k_{cat}/K_m)_{E\cdot HP_i} = 185$ M^{-1} s^{-1}].

The free energy change $\Delta G_o = -5.8$ kcal/mol for binding of phosphite dianion to the binary complex $E\cdot S^{\ddagger}$ represents the total intrinsic binding energy of exogenous phosphite dianion available from its interactions with the protein at the transition state complex (Figure 5A). There should be no direct *stabilizing* interactions between bound phosphite dianion and the altered substrate in the transition state at the $E\cdot HPO_3^{2-}\cdot S^{\ddagger}$ complex; any simple interaction of the negatively charged phosphite dianion with the negative charge at the developing enediolate intermediate would be expected to be *destabilizing*. Therefore, the smaller value of $\Delta G_o = -1.9$ kcal/mol observed for the binding of phosphite dianion in the ground state strongly suggests that the binding of phosphite dianion to the free enzyme is accompanied by a second unfavorable process with a free energy change of +3.9 kcal/mol.

Origin and Economics of Catalysis of Proton Transfer by TIM. Crystallographic studies show that TIM exists predominantly in a "loop open" conformation in the absence of bound ligands but that the binding of phosphodianion ligands such as the transition state/intermediate analogues PGA (*36*, *44*) and phosphoglycolohydroxamate (*37*, *42*, *45*), the substrate analogue glycerol 3-phosphate (*38*), and the substrate DHAP (*34*, *43*) is accompanied by a large conformational change (*71*). At a *minimum*, this includes a ca. 7 Å movement of the 11-residue mobile loop (loop 6) to close over the mouth of the active site which results in formation of a hydrogen bond between the backbone amide NH group

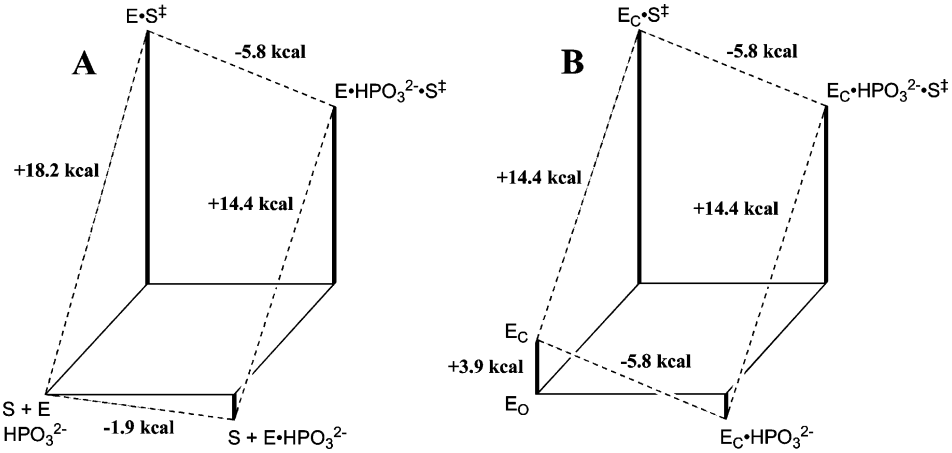

FIGURE 5: (A) Free energy profiles for turnover of glycolaldehyde (S) by free TIM (E) and by TIM that is saturated with phosphite dianion ($E{\cdot}HPO_3^{2-}$). Activation free energy changes were calculated using the Eyring equation at 298 K. The observed tighter binding of phosphite dianion to the transition state complex $E{\cdot}S^{\ddagger}$ ($\Delta G_o = -5.8$ kcal/mol) than to the free enzyme E ($\Delta G_o = -1.9$ kcal/mol) represents the "interaction energy" of 3.9 kcal/mol (*76*, *77*). (B) The *difference* between the total intrinsic binding energy of −5.8 kcal/mol and the observed free energy change of −1.9 kcal/mol for binding of phosphite dianion to the *inactive open* ground state enzyme E_O to give the *active closed* liganded enzyme $E_C{\cdot}HPO_3^{2-}$ can be attributed to $\Delta G_{conf} = 3.9$ kcal/mol for an unfavorable conformational change that converts E_O to the *active closed* enzyme E_C. The observed value of $\Delta G^{\ddagger} = 18.2$ kcal/mol for turnover of glycolaldehyde (Figure 5A) may be partitioned conceptually into $\Delta G^{\ddagger} = 14.4$ kcal/mol for proton transfer from glycolaldehyde to E_C and $\Delta G_{conf} = 3.9$ kcal/mol for the obligate unfavorable conformational change that converts E_O to E_C.

of Gly-171 at the tip of the loop and an anionic oxygen of the bound phosphodianion group (*36*−*38*, *40*−*42*, *44*, *45*). Importantly, ligand binding and loop closing are also accompanied by a 2−3 Å movement of the side chain of the catalytic base Glu-165 toward the bound ligand, from a "swung-out" to a "swung-in" position (*36*, *37*, *40*, *42*, *45*, *78*). This movement of Glu-165 places an oxygen of its carboxylate group between C1 and C2 of bound dihydroxyacetone phosphate where it is optimally aligned for proton transfer (*43*). There is crystallographic evidence that the binding of phosphate dianion to trypanosomal TIM results in a "loop closed" conformation in which this simple inorganic oxydianion occupies the same binding site with the same protein−ligand contacts that are observed for the phosphodianion group of bound glycerol 3-phosphate (*79*). Moreover, the binding of phosphate dianion is also accompanied by the movement of Glu-165 into the active swung-in position that is observed for TIM complexed with phosphodianion substrate and intermediate analogues (*79*). By analogy, the binding of phosphite dianion to TIM should also result in a substantial conformational change, involving closing of the mobile loop over the active site, the formation of a hydrogen bond between the backbone amide NH group of Gly-171 and the phosphite ligand, and the movement of Glu-165 into the active swung-in position where it would be positioned for abstraction of a proton from co-bound glycolaldehyde.

We propose that a large portion of the intrinsic binding energy of phosphite dianion is used to drive a conformational change from an *inactive open* form of TIM that is not competent for proton transfer to an *active closed* form of the enzyme at which the active site is organized for optimal stabilization of the transition state for proton transfer from bound substrate. This organization would involve the repositioning of Glu-165 into a conformation that is optimal for proton transfer from bound substrate, along with the exclusion of solvent from the active site cavity which in turn would lower its effective dielectric constant. Crystallographic studies show that loop closing and the repositioning of Glu-165 result in a 3−4 Å movement of its carboxylate group toward Leu-230 in loop 8 (*44*, *78*), along with a 3 Å movement of Ile-170 in loop 6 deeper into the active site toward Glu-165 (*39*, *40*). Thus loop closing and reorganization of the active site place the anionic carboxylate group of Glu-165 into close proximity with the bulky hydrophobic side chains of the conserved residues Ile-170 and Leu-230 (*38*−*40*, *43*, *44*, *78*). We propose that this makes a major contribution to the observed ca. 3 unit higher pK_a of Glu-165 in the complex with 2-phosphoglycolate than at the free enzyme (*22*, *80*), which in turn serves to increase the driving force for proton transfer (*81*). The placement of Glu-165 in a hydrophobic environment provides a strong driving force for proton transfer from bound substrate because this moves essentially localized negative charge from a highly hydrophobic environment onto the enolic oxygen of the enediolate intermediate. Stabilization of negative charge at the enediolate by electrostatic and/or hydrogen bonding interactions with His-95 and Lys-12 is strongly favored by the low effective dielectric constant of the active site that arises from the exclusion of water and the proximity of Ile-170 and Leu-230 (*6*, *82*).

The "economics" of our model for catalysis by TIM are illustrated in Figure 5B (*77*). In this model, both phosphite dianion and the altered substrate in the transition state stabilize the same *active closed* form of the enzyme, E_C. The difference between the total intrinsic binding energy of −5.8 kcal/mol and the observed free energy change of −1.9 kcal/mol for binding of phosphite dianion to the *inactive open* ground state enzyme E_O to give the *active closed* liganded enzyme $E_C{\cdot}HPO_3^{2-}$ can be attributed to $\Delta G_{conf} = 3.9$ kcal/mol for an obligate unfavorable conformational change that converts the open enzyme E_O to the closed enzyme E_C and results in reorganization of the active site as described above (*77*, *83*). We propose that the reactivity of the *active closed* enzyme E_C toward bound substrate is essentially independent of the presence of bound phosphite dianion. Therefore, the observed value of $\Delta G^{\ddagger} = +18.2$ kcal/mol for turnover of glycolaldehyde (Figure 5A) may be conceptually partitioned

into $\Delta G^{\ddagger} = +14.4$ kcal/mol for proton transfer from glycolaldehyde to the *active closed* enzyme and $\Delta G_{conf} = +3.9$ kcal/mol for the conformational change from the *inactive open* to the *active closed* enzyme that must occur to facilitate proton transfer (Figure 5B). Furthermore, this model accounts for the observation that the binary complexes $E_C{\cdot}S^{\ddagger}$ and $E_C{\cdot}HPO_3^{2-}$ exhibit much higher affinities for HPO_3^{2-} and the altered substrate in the transition state, respectively, because the binding of $S^{\ddagger}$ or of HPO_3^{2-} results in a conformational change to the closed enzyme at which full intrinsic binding energies may be expressed upon subsequent ligand binding to give a ternary complex.

The values of K_m for turnover of glycolaldehyde by the free enzyme and the $E{\cdot}HPO_3^{2-}$ complex should be very similar because the binding interactions of this simple two-carbon sugar with the enzyme should be largely confined to those with His-95 and Lys-12, whose positions do not change significantly upon closure of the mobile loop (*36*, *40*). Therefore, the 700-fold larger value of k_{cat}/K_m for turnover of glycolaldehyde by the binary complex $E{\cdot}HPO_3^{2-}$ than by free TIM likely also translates to a 700-fold larger value of k_{cat} for $E{\cdot}HPO_3^{2-}$. In this case, the intrinsic binding energy of phosphite dianion is used *directly* to increase the rate constant for proton transfer from bound substrate to the enzyme.

Comparison of Phosphite and Phosphate Dianions. Scheme 7 shows that the α-hydroxycarbonyl and inorganic oxydianion "pieces" of GAP are modeled by the minimal two-carbon sugar glycolaldehyde and phosphite dianion. Truncation of both the sugar and the formal phosphate dianion portions of the substrate is necessary for generation of a "two-part substrate" that maintains the same approximate steric bulk of the "holistic substrate" (*84*).

Scheme 7

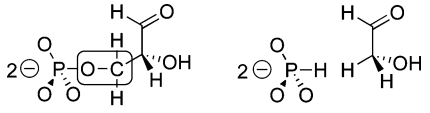

The value of $k_{obsd} = 2.9 \times 10^{-6}$ s^{-1} for turnover of *h*-GLY by 42 μM TIM in the presence of 15 mM phosphate dianion can be corrected for the nonspecific reaction that occurs outside the active site ($k_{non} = 0.0106$ M^{-1} s^{-1}) and the presence of 6.1% of the free carbonyl form of glycolaldehyde to give $(k_{cat}/K_m)_{obsd} = 0.96$ M^{-1} s^{-1}. This is only 3.7-fold larger than $(k_{cat}/K_m)_E = 0.26$ M^{-1} s^{-1} for turnover of *h*-GLY by TIM in the absence of phosphate dianion (Table 1). By contrast, the addition of 15 mM phosphite dianion results in a 200-fold increase in $(k_{cat}/K_m)_{obsd}$ for the turnover of *h*-GLY (Table 1). The value of $K_i = 13$ mM for competitive inhibition of TIM by phosphate dianion in H_2O at pH 7.4 ($I = 0.12$) is 2.2-fold smaller than $K_i = 29$ mM for phosphite dianion under the same conditions (this work). These data, together with $K_d = 38$ mM for phosphite dianion in D_2O, can be used to estimate a value of $K_d = 17$ mM for binding of phosphate dianion to TIM in D_2O at pD 7.0 ($I = 0.10$). Therefore, the value of $(k_{cat}/K_m)_{obsd} = 0.96$ M^{-1} s^{-1} can be substituted into eq 6 rewritten for phosphate dianion with $K_d = 17$ mM to give $(k_{cat}/K_m)_{E{\cdot}P_i} \approx 1.7$ M^{-1} s^{-1} as the second-order rate constant for turnover of *h*-GLY by TIM that is saturated with phosphate dianion. This is 100-fold smaller than $(k_{cat}/K_m)_{E{\cdot}HP_i} = 185$ M^{-1} s^{-1} for TIM that is saturated with phosphite dianion. Therefore, there is a large sensitivity of the reactivity of TIM toward proton transfer from glycolaldehyde to the steric and electronic properties of the co-bound oxydianion activator (*85*). Replacement of the H group at phosphite dianion with the larger OH group to give phosphate dianion may prevent the correct productive co-binding of both glycolaldehyde and the oxydianion in the active site. This could result in incomplete or incorrect closing of the mobile loop and an active site environment that is less than optimal for catalysis of proton transfer. There may also be unfavorable electrostatic consequences, for example, an unfavorable interaction of the positive dipole of the OH group at bound phosphate dianion with the positive charge of Lys-12 in the active site.

Utilization of the Intrinsic Binding Energy of the Remote Substrate Phosphodianion Group: A General Strategy for Enzymatic Catalysis? Our earlier comparison of the TIM-catalyzed reactions of the neutral triose (*R*)-glyceraldehyde and GAP showed that the total intrinsic binding energy of the substrate phosphodianion group in the transition state for proton transfer, calculated from the ratio of the second-order rate constants for turnover of GAP and (*R*)-glyceraldehyde, is 14.1 kcal/mol (*62*). The large intrinsic binding energy for exogenous phosphite dianion in the transition state for deprotonation of glycolaldehyde (5.8 kcal/mol) shows that a significant fraction of the transition state stabilization due to the phosphodianion group at GAP can be "reconstituted" by binding a small oxydianion ligand to TIM. The remaining ca. 8 kcal/mol may be attributed to several factors.

(1) The entropic price for binding phosphite dianion to the binary complex $E{\cdot}S^{\ddagger}$ to give the ternary complex $E{\cdot}S^{\ddagger}{\cdot}HPO_3^{2-}$. This price does not have to be "paid" by the intramolecular phosphodianion group which is already present at the binary transition state complex for the reaction of GAP. The moderate value of 8 kcal/mol is considerably less than the estimated maximal value of 11−12 kcal/mol (*76*, *86*).

(2) The separate binding of glycolaldehyde and phosphite dianion may result in incomplete or incorrect closure of the mobile loop such that the active site environment is not completely optimized for catalysis of proton transfer.

(3) The combination of the enediolate intermediate generated from deprotonation of glycolaldehyde and phosphite dianion is unlikely to be a perfect steric and electronic match for the enzyme-bound enediolate intermediate generated by deprotonation of GAP. Small differences in the steric and/or electrostatic and hydrogen bonding interactions of the two fragments with the enzyme in the transition state, compared with those for the reaction of GAP, could result in less than optimal stabilization of the intermediate and a corresponding destabilization of the transition state for its formation.

(4) A potentially important interaction between Lys-12 and the bridging oxygen of the substrate phosphodianion group has been identified in the crystal structure of the Michaelis complex of yeast TIM with DHAP (*43*). It has also been observed that the TIM-catalyzed isomerization of the phosphonate analogue of GAP, (*R*)-2-hydroxy-4-phosphonobutyraldehyde, is 800-fold slower than that of GAP (*21*). By analogy, the absence of this bridging oxygen may

reduce $(k_{cat}/K_m)_{E\cdot HP_i}$ for turnover of glycolaldehyde by the TIM·HPO_3^{2-} complex.

In parallel with the work described here, we have shown that the binding of phosphite dianion to orotidine 5′-monophosphate decarboxylase (OMPDC) stabilizes the transition state for decarboxylation of a neutral truncated substrate that lacks the 5′-phosphodianion group of the natural substrate by 7.8 kcal/mol (*87*). TIM and OMPDC have come to represent paradigms for enzyme-catalyzed proton transfer and decarboxylation reactions, respectively. OMPDC is the titular member of the OMPDC "suprafamily" (*28*, *88*, *89*) and shares the ubiquitous $(\beta,\alpha)_8$-barrel fold that was first observed for TIM (*90*, *91*), along with a common canonical phosphate binding site at loops 7 and 8 (*28*, *29*, *88*). Moreover, both TIM and OMPDC are characterized by interactions of flexible loop(s) with the phosphodianion group of bound ligands (loop 6 for TIM and loop 7 for OMPDC) (*90*, *91*), the closure of which sequesters the bound substrate from bulk solvent. It is possible that the utilization by these enzymes of the intrinsic binding energy of the remote phosphodianion group of the substrate for transition state stabilization is a coincidence, and of limited general significance. However, we propose that the interactions of the closed flexible loops of TIM and OMPDC with the substrate phosphodianion group represent a common strategy that enables efficient recruitment of the intrinsic binding energy of a small remote binding determinant for transition state stabilization. By contrast with TIM, the mechanism of action of the extraordinarily efficient OMPDC remains largely undefined. Further studies aimed at elucidating the structural and dynamic strategies used to elicit its enormous 10^{17}-fold rate acceleration (*92*) are clearly warranted.

REFERENCES

1. Gerlt, J. A. (2007) Enzymatic Catalysis of Proton Transfer at Carbon Atoms, in *Hydrogen-Transfer Reactions, Volume 3, Biological Aspects I-II* (Hynes, J. T., Klinman, J. P., Limbach, H.-H., and Schowen, R. L., Eds.) pp 1107−1137, Wiley-VCH, Weinheim, Germany.
2. Gerlt, J. A., Babbitt, P. C., and Rayment, I. (2005) Divergent evolution in the enolase superfamily: The interplay of mechanism and specificity, *Arch. Biochem. Biophys. 433*, 59−70.
3. Pollack, R. M. (2004) Enzymatic mechanisms for catalysis of enolization: Ketosteroid isomerase, *Bioorg. Chem. 32*, 341−353.
4. Kenyon, G. L., Gerlt, J. A., Petsko, G. A., and Kozarich, J. W. (1995) Mandelate Racemase: Structure-Function Studies of a Pseudosymmetric Enzyme, *Acc. Chem. Res. 28*, 178−186.
5. Amyes, T. L., and Richard, J. P. (2007) Proton Transfer to and from Carbon in Model Systems, in *Hydrogen-Transfer Reactions, Volume 3, Biological Aspects I-II* (Hynes, J. T., Klinman, J. P., Limbach, H.-H., and Schowen, R. L., Eds.) pp 949−973, Wiley-VCH, Weinheim, Germany.
6. Richard, J. P., and Amyes, T. L. (2001) Proton Transfer at Carbon, *Curr. Opin. Chem. Biol. 5*, 626−633.
7. Gerlt, J. A., and Gassman, P. G. (1993) Understanding the rates of certain enzyme-catalyzed reactions: Proton abstraction from carbon acids, acyl transfer reactions, and displacement reactions of phosphodiesters, *Biochemistry 32*, 11943−11952.
8. Rieder, S. V., and Rose, I. A. (1959) Mechanism of the triose phosphate isomerase reaction, *J. Biol. Chem. 234*, 1007−1010.
9. Knowles, J. R. (1991) Enzyme catalysis: Not different, just better, *Nature 350*, 121−124.
10. Knowles, J. R. (1991) To build an enzyme, *Philos. Trans. R. Soc. London, Ser. B 332*, 115−121.
11. Knowles, J. R., and Albery, W. J. (1977) Perfection in enzyme catalysis: The energetics of triosephosphate isomerase, *Acc. Chem. Res. 10*, 105−111.
12. Miller, J. C., and Waley, S. G. (1971) Active center of rabbit muscle triose phosphate isomerase. Site that is labeled by glycidol phosphate, *Biochem. J. 123*, 163−170.
13. Hartman, F. C. (1971) Haloacetol phosphates. Characterization of the active site of rabbit muscle triose phosphate isomerase, *Biochemistry 10*, 146−154.
14. De la Mare, S., Coulson, A. F. W., Knowles, J. R., Priddle, J. D., and Offord, R. E. (1972) Active-site labeling of triose phosphate isomerase. Reaction of bromohydroxyacetone phosphate with a unique glutamic acid residue and the migration of the label to tyrosine, *Biochem. J. 129*, 321−331.
15. Lodi, P. J., and Knowles, J. R. (1991) Neutral imidazole is the electrophile in the reaction catalyzed by triosephosphate isomerase: Structural origins and catalytic implications, *Biochemistry 30*, 6948−6956.
16. Campbell, I. D., Jones, R. B., Kiener, P. A., and Waley, S. G. (1979) Enzyme-substrate and enzyme-inhibitor complexes of triose phosphate isomerase studied by ^{31}P nuclear magnetic resonance, *Biochem. J. 179*, 607−621.
17. Webb, M. R., Standring, D. N., and Knowles, J. R. (1977) Phosphorus-31 nuclear magnetic resonance of dihydroxyacetone phosphate in the presence of triosephosphate isomerase. The question of nonproductive binding of the substrate hydrate, *Biochemistry 16*, 2738−2741.
18. Komives, E. A., Chang, L. C., Lolis, E., Tilton, R. F., Petsko, G. A., and Knowles, J. R. (1991) Electrophilic catalysis in triosephosphate isomerase: The role of histidine-95, *Biochemistry 30*, 3011−3019.
19. Putman, S. J., Coulson, A. F. W., Farley, I. R. T., Riddleston, B., and Knowles, J. R. (1972) Specificity and kinetics of triose phosphate isomerase from chicken muscle, *Biochem. J. 129*, 301−310.
20. Plaut, B., and Knowles, J. R. (1972) pH-Dependence of the triose phosphate isomerase reaction, *Biochem. J. 129*, 311−320.
21. Belasco, J. G., Herlihy, J. M., and Knowles, J. R. (1978) Critical ionization states in the reaction catalyzed by triosephosphate isomerase, *Biochemistry 17*, 2971−2978.
22. Hartman, F. C., LaMuraglia, G. M., Tomozawa, Y., and Wolfenden, R. (1975) The influence of pH on the interaction of inhibitors with triosephosphate isomerase and determination of the pK_a of the active-site carboxyl group, *Biochemistry 14*, 5274−5279.
23. Hartman, F. C., and Ratrie, H., III (1977) Apparent equivalence of the active-site glutamyl residue and the essential group with pK_a 6.0 in triosephosphate isomerase, *Biochem. Biophys. Res. Commun. 77*, 746−752.
24. O'Donoghue, A. C., Amyes, T. L., and Richard, J. P. (2005) Hydron Transfer Catalyzed by Triosephosphate Isomerase. Products of Isomerization of Dihydroxyacetone Phosphate in D_2O, *Biochemistry 44*, 2622−2631.
25. O'Donoghue, A. C., Amyes, T. L., and Richard, J. P. (2005) Hydron Transfer Catalyzed by Triosephosphate Isomerase. Products of Isomerization of (*R*)-Glyceraldehyde 3-Phosphate in D_2O, *Biochemistry 44*, 2610−2621.
26. Harris, T. K., Cole, R. N., Comer, F. I., and Mildvan, A. S. (1998) Proton Transfer in the Mechanism of Triosephosphate Isomerase, *Biochemistry 37*, 16828−16838.
27. Rose, I. A., Fung, W. J., and Warms, J. V. B. (1990) Proton diffusion in the active site of triosephosphate isomerase, *Biochemistry 29*, 4312−4317.
28. Gerlt, J. A., and Raushel, F. M. (2003) Evolution of function in $(\beta/\alpha)_8$-barrel enzymes, *Curr. Opin. Chem. Biol. 7*, 252−264.
29. Nagano, N., Orengo, C. A., and Thornton, J. M. (2002) One fold with many functions: The evolutionary relationships between TIM barrel families based on their sequences, structures and functions, *J. Mol. Biol. 321*, 741−765.
30. Wierenga, R. K. (2001) The TIM-barrel fold: A versatile framework for efficient enzymes, *FEBS Lett. 492*, 193−198.
31. Lodi, P. J., Chang, L. C., Knowles, J. R., and Komives, E. A. (1994) Triosephosphate Isomerase Requires a Positively Charged Active Site: The Role of Lysine-12, *Biochemistry 33*, 2809−2814.
32. Nickbarg, E. B., Davenport, R. C., Petsko, G. A., and Knowles, J. R. (1988) Triosephosphate isomerase: Removal of a putatively electrophilic histidine residue results in a subtle change in catalytic mechanism, *Biochemistry 27*, 5948−5960.
33. Straus, D., Raines, R., Kawashima, E., Knowles, J. R., and Gilbert, W. (1985) Active site of triosephosphate isomerase: In vitro mutagenesis and characterization of an altered enzyme, *Proc. Natl. Acad. Sci. U.S.A. 82*, 2272−2276.

34. Alber, T., Banner, D. W., Bloomer, A. C., Petsko, G. A., Phillips, D., Rivers, P. S., and Wilson, I. A. (1981) On the three-dimensional structure and catalytic mechanism of triose phosphate isomerase, *Philos. Trans. R. Soc. London, Ser. B 293*, 159−171.
35. Lolis, E., Alber, T., Davenport, R. C., Rose, D., Hartman, F. C., and Petsko, G. A. (1990) Structure of yeast triosephosphate isomerase at 1.9-Å resolution, *Biochemistry 29*, 6609−6618.
36. Lolis, E., and Petsko, G. A. (1990) Crystallographic analysis of the complex between triosephosphate isomerase and 2-phosphoglycolate at 2.5-Å resolution: Implications for catalysis, *Biochemistry 29*, 6619−6625.
37. Davenport, R. C., Bash, P. A., Seaton, B. A., Karplus, M., Petsko, G. A., and Ringe, D. (1991) Structure of the triosephosphate isomerase-phosphoglycolohydroxamate complex: An analog of the intermediate on the reaction pathway, *Biochemistry 30*, 5821−5826.
38. Noble, M. E. M., Wierenga, R. K., Lambeir, A. M., Opperdoes, F. R., Thunnissen, A. M. W. H., Kalk, K. H., Groendijk, H., and Hol, W. G. J. (1991) The adaptability of the active site of trypanosomal triosephosphate isomerase as observed in the crystal structures of three different complexes, *Proteins: Struct., Funct., Genet. 10*, 50−69.
39. Wierenga, R. K., Noble, M. E. M., Vriend, G., Nauche, S., and Hol, W. G. J. (1991) Refined 1.83 Å structure of trypanosomal triosephosphate isomerase crystallized in the presence of 2.4 M ammonium sulfate. A comparison with the structure of the trypanosomal triosephosphate isomerase-glycerol-3-phosphate complex, *J. Mol. Biol. 220*, 995−1015.
40. Wierenga, R. K., Borchert, T. V., and Noble, M. E. M. (1992) Crystallographic binding studies with triosephosphate isomerases: Conformational changes induced by substrate and substrate analogs, *FEBS Lett. 307*, 34−39.
41. Wierenga, R. K., Noble, M. E. M., and Davenport, R. C. (1992) Comparison of the refined crystal structures of liganded and unliganded chicken, yeast and trypanosomal triosephosphate isomerase, *J. Mol. Biol. 224*, 1115−1126.
42. Zhang, Z., Sugio, S., Komives, E. A., Liu, K. D., Knowles, J. R., Petsko, G. A., and Ringe, D. (1994) Crystal Structure of Recombinant Chicken Triosephosphate Isomerase-Phosphoglycolohydroxamate Complex at 1.8-Å Resolution, *Biochemistry 33*, 2830−2837.
43. Jogl, G., Rozovsky, S., McDermott, A. E., and Tong, L. (2003) Optimal alignment for enzymatic proton transfer: Structure of the Michaelis complex of triosephosphate isomerase at 1.2 Å resolution, *Proc. Natl. Acad. Sci. U.S.A. 100*, 50−55.
44. Kursula, I., and Wierenga, R. K. (2003) Crystal structure of triosephosphate isomerase complexed with 2-phosphoglycolate at 0.83-Å resolution, *J. Biol. Chem. 278*, 9544−9551.
45. Noble, M. E. M., Zeelen, J. P., and Wierenga, R. K. (1993) Structures of the "open" and "closed" state of trypanosomal triosephosphate isomerase, as observed in a new crystal form: Implications for the reaction mechanism, *Proteins: Struct., Funct., Genet. 16*, 311−326.
46. Pompliano, D. L., Peyman, A., and Knowles, J. R. (1990) Stabilization of a reaction intermediate as a catalytic device: Definition of the functional role of the flexible loop in triosephosphate isomerase, *Biochemistry 29*, 3186−3194.
47. Sampson, N. S., and Knowles, J. R. (1992) Segmental movement: Definition of the structural requirements for loop closure in catalysis by triosephosphate isomerase, *Biochemistry 31*, 8482−8487.
48. Sampson, N. S., and Knowles, J. R. (1992) Segmental motion in catalysis: Investigation of a hydrogen bond critical for loop closure in the reaction of triosephosphate isomerase, *Biochemistry 31*, 8488−8494.
49. Sun, J., and Sampson, N. S. (1999) Understanding Protein Lids: Kinetic Analysis of Active Hinge Mutants in Triosephosphate Isomerase, *Biochemistry 38*, 11474−11481.
50. Xiang, J., Sun, J., and Sampson, N. S. (2001) The Importance of Hinge Sequence for Loop Function and Catalytic Activity in the Reaction Catalyzed by Triosephosphate Isomerase, *J. Mol. Biol. 307*, 1103−1112.
51. Xiang, J., Jung, J.-y., and Sampson, N. S. (2004) Entropy effects on protein hinges: The reaction catalyzed by triosephosphate isomerase, *Biochemistry 43*, 11436−11445.
52. Massi, F., Wang, C., and Palmer, A. G., III (2006) Solution NMR and computer simulation studies of active site loop motion in triosephosphate isomerase, *Biochemistry 45*, 10787−10794.
53. Kurkcuoglu, O., Jernigan, R. L., and Doruker, P. (2006) Loop motions of triosephosphate isomerase observed with elastic networks, *Biochemistry 45*, 1173−1182.
54. Guallar, V., Jacobson, M., McDermott, A., and Friesner, R. A. (2004) Computational Modeling of the Catalytic Reaction in Triosephosphate Isomerase, *J. Mol. Biol. 337*, 227−239.
55. Derreumaux, P., and Schlick, T. (1998) The loop opening/closing motion of the enzyme triosephosphate isomerase, *Biophys. J. 74*, 72−81.
56. Joseph, D., Petsko, G. A., and Karplus, M. (1990) Anatomy of a conformational change: Hinged "lid" motion of the triosephosphate isomerase loop, *Science 249*, 1425−1428.
57. Rozovsky, S., Jogl, G., Tong, L., and McDermott, A. E. (2001) Solution-state NMR investigations of triosephosphate isomerase active site loop motion: Ligand release in relation to active site loop dynamics, *J. Mol. Biol. 310*, 271−280.
58. Rozovsky, S., and McDermott, A. E. (2001) The time scale of the catalytic loop motion in triosephosphate isomerase, *J. Mol. Biol. 310*, 259−270.
59. Desamero, R., Rozovsky, S., Zhadin, N., McDermott, A., and Callender, R. (2003) Active Site Loop Motion in Triosephosphate Isomerase: T-Jump Relaxation Spectroscopy of Thermal Activation, *Biochemistry 42*, 2941−2951.
60. Norledge, B. V., Lambeir, A. M., Abagyan, R. A., Rottmann, A., Fernandez, A. M., Filimonov, V. V., Peter, M. G., and Wierenga, R. K. (2001) Modeling, mutagenesis, and structural studies on the fully conserved phosphate-binding loop (loop 8) of triosephosphate isomerase: Toward a new substrate specificity, *Proteins: Struct., Funct., Genet. 42*, 383−389.
61. Richard, J. P. (1984) Acid-base catalysis of the elimination and isomerization reactions of triose phosphates, *J. Am. Chem. Soc. 106*, 4926−4936.
62. Amyes, T. L., O'Donoghue, A. C., and Richard, J. P. (2001) Contribution of phosphate intrinsic binding energy to the enzymatic rate acceleration for triosephosphate isomerase, *J. Am. Chem. Soc. 123*, 11325−11326.
63. Collins, G. C. S., and George, W. O. (1971) Nuclear Magnetic Resonance Spectra of Glycolaldehyde, *J. Chem. Soc. B*, 1352−1355.
64. Glushonok, G. K., Petryaev, E. P., Turetskaya, E. A., and Shadyro, O. I. (1986) Equilibrium between the Molecular Forms of Glycolaldehyde and DL-Glyceraldehyde in Aqueous Solutions, *Russ. J. Phys. Chem. 60*, 1788−1794.
65. Glasoe, P. K., and Long, F. A. (1960) Use of glass electrodes to measure acidities in deuterium oxide, *J. Phys. Chem. 64*, 188−190.
66. Krietsch, W. K. G., Pentchev, P. G., Klingenbuerg, H., Hofstaetter, T., and Buecher, T. (1970) Isolation and crystallization of yeast and rabbit liver triose phosphate isomerase and a comparative characterization with the rabbit muscle enzyme, *Eur. J. Biochem. 14*, 289−300.
67. Raiford, D. S., Fisk, C. L., and Becker, E. D. (1979) Calibration of methanol and ethylene glycol nuclear magnetic resonance thermometers, *Anal. Chem. 51*, 2050−2051.
68. Nagorski, R. W., and Richard, J. P. (2001) Mechanistic Imperatives for Aldose-Ketose Isomerization in Water: Specific, General Base- and Metal Ion-Catalyzed Isomerization of Glyceraldehyde with Proton and Hydride Transfer, *J. Am. Chem. Soc. 123*, 794−802.
69. Nagorski, R. W., and Richard, J. P. (1996) Mechanistic Imperatives for Enzymatic Catalysis of Aldose-Ketose Isomerization: Isomerization of Glyceraldehyde in Weakly Alkaline Solution Occurs with Intramolecular Transfer of a Hydride Ion, *J. Am. Chem. Soc. 118*, 7432−7433.
70. Crugeiras, J., and Richard, J. P. (2004) A Comparison of the Electrophilic Reactivities of Zn^{2+} and Acetic Acid as Catalysts of Enolization: Imperatives for Enzymatic Catalysis of Proton Transfer at Carbon, *J. Am. Chem. Soc. 126*, 5164−5173.
71. Johnson, L. N., and Wolfenden, R. (1970) Changes in absorption spectrum and crystal structure of triose phosphate isomerase brought about by 2-phosphoglycollate, a potential transition state analog, *J. Mol. Biol. 47*, 93−100.
72. Davis, L. (1973) Structure of dihydroxyacetone in solution, *Bioorg. Chem. 2*, 197−201.
73. Glushonok, G. K., Glushonok, T. G., Maslovskaya, L. A., and Shadyro, O. I. (2003) A ^{1}H and ^{13}C NMR and UV Study of the State of Hydroxyacetone in Aqueous Solutions**,** *Russ. J. Gen. Chem. 73*, 1027−1031.

74. Glomb, M. A., and Monnier, V. M. (1995) Mechanism of protein modification by glyoxal and glycolaldehyde, reactive intermediates of the Maillard reaction, *J. Biol. Chem. 270*, 10017−10026.
75. Thornalley, P. J., Langborg, A., and Minhas, H. S. (1999) Formation of glyoxal, methylglyoxal and 3-deoxyglucosone in the glycation of proteins by glucose, *Biochem. J. 344*, 109−116.
76. Jencks, W. P. (1981) On the attribution and additivity of binding energies, *Proc. Natl. Acad. Sci. U.S.A. 78*, 4046−4050.
77. Jencks, W. P. (1987) Economics of enzyme catalysis, *Cold Spring Harbor Symp. Quant. Biol. 52*, 65−73.
78. Kursula, I., Partanen, S., Lambeir, A.-M., Antonov, D. M., Augustyns, K., and Wierenga, R. K. (2001) Structural determinants for ligand binding and catalysis of triosephosphate isomerase, *Eur. J. Biochem. 268*, 5189−5196.
79. Verlinde, C. L. M. J., Noble, M. E. M., Kalk, K. H., Groendijk, H., Wierenga, R. K., and Hol, W. G. J. (1991) Anion binding at the active site of trypanosomal triosephosphate isomerase. Monohydrogen phosphate does not mimic sulfate, *Eur. J. Biochem. 198*, 53−57.
80. Campbell, I. D., Jones, R. B., Kiener, P. A., Richards, E., Waley, S. C., and Wolfenden, R. (1978) The form of 2-phosphoglycollic acid bound by triosephosphate isomerase, *Biochem. Biophys. Res. Commun. 83*, 347−352.
81. Richard, J. P. (1998) The Enhancement of Enzymic Rate Accelerations by Brønsted Acid-Base Catalysis, *Biochemistry 37*, 4305−4309.
82. Richard, J. P., and Amyes, T. L. (2004) On the importance of being zwitterionic: Enzymic catalysis of decarboxylation and deprotonation of cationic carbon, *Bioorg. Chem. 32*, 354−366.
83. Jencks, W. P. (1975) Binding Energy, Specificity and Enzymic Catalysis: The Circe Effect, *Adv. Enzymol. Relat. Areas Mol. Biol. 43*, 219−410.
84. Ray, W. J., Jr., and Long, J. W. (1976) Thermodynamics and mechanism of the PO_3 transfer process in the phosphoglucomutase reaction, *Biochemistry 15*, 3993−4006.
85. Ray, W. J., Jr., Long, J. W., and Owens, J. D. (1976) An analysis of the substrate-induced rate effect in the phosphoglucomutase system, *Biochemistry 15*, 4006−4017.
86. Page, M. I., and Jencks, W. P. (1971) Entropic contributions to rate accelerations in enzymic and intramolecular reactions and the chelate effect, *Proc. Natl. Acad. Sci. U.S.A. 68*, 1678−1683.
87. Amyes, T. L., Richard, J. P., and Tait, J. J. (2005) Activation of Orotidine 5′-Monophosphate Decarboxylase by Phosphite Dianion: The Whole Substrate is the Sum of Two Parts, *J. Am. Chem. Soc. 127*, 15708−15709.
88. Wise, E., Yew, W. S., Babbitt, P. C., Gerlt, J. A., and Rayment, I. (2002) Homologous $(\beta/\alpha)_8$-Barrel Enzymes That Catalyze Unrelated Reactions: Orotidine 5′-Monophosphate Decarboxylase and 3-Keto-L-gulonate 6-Phosphate Decarboxylase, *Biochemistry 41*, 3861−3869.
89. Gerlt, J. A., and Babbitt, P. C. (2001) Divergent evolution of enzymatic function: Mechanistically diverse superfamilies and functionally distinct suprafamilies, *Annu. Rev. Biochem. 70*, 209−246.
90. Begley, T. P., Appleby, T. C., and Ealick, S. E. (2000) The structural basis for the remarkable catalytic proficiency of orotidine 5′-monophosphate decarboxylase, *Curr. Opin. Struct. Biol. 10*, 711−718.
91. Miller, B. G., Hassell, A. M., Wolfenden, R., Milburn, M. V., and Short, S. A. (2000) Anatomy of a proficient enzyme: The structure of orotidine 5′-monophosphate decarboxylase in the presence and absence of a potential transition state analog, *Proc. Natl. Acad. Sci. U.S.A. 97*, 2011−2016.
92. Radzicka, A., and Wolfenden, R. (1995) A proficient enzyme, *Science 267*, 90−93.
93. Jones, J. M., and Bender, M. L. (1960) Secondary deuterium isotope effects in the addition equilibria of ketones, *J. Am. Chem. Soc. 82*, 6322−6326

BI700409B